ARTICLE

The copper sulfate hydration cycle. Crystal structures of $CuSO_4$ (Chalcocyanite), $CuSO_4·H_2O$ (Poitevinite), $CuSO_4·3H_2O$ (Bonattite) and $CuSO_4·5H_2O$ (Chalcanthite) at low temperature using non-spherical atomic scattering factors†

Received 00th January 20xx,
Accepted 00th January 20xx

DOI: 10.1039/x0xx00000x

Mukaila A. Ibrahim [a,b] and René T. Boeré* [a,b]

New structure determinations of $CuSO_4$, $CuSO_4·H_2O$, $CuSO_4·3H_2O$ and $CuSO_4·5H_2O$, are reported from X-ray diffraction experiments at 100 (1) K. Combined density functional theory (ORCA) and non-spherical atomic scattering factor (NoSpherA2) computations enabled a Hirshfeld Atom Refinement (HAR) using custom atom scattering factors, accurately polarized and charge-compensated atom electron densities and accurate placement and shapes of the water hydrogen atoms. The results clearly demonstrate that all H atoms are involved in conventional H-bonding in the structures of the hydrates, contrary to an early X-ray diffraction determination on $CuSO_4·3H_2O$. Comparison to neutron diffraction results demonstrates the efficacy of this new HAR method. Colour variation in copper sulfates is interpretable by considering the relative number of sulfato and aqua ligands, given the lower crystal field splitting of the former relative to the latter.

Introduction

'Simple' compounds of copper(II) such as chlorides and sulfates are ubiquitous in chemistry, technology, and mineralogy. Perhaps the best known is the intensely blue pentahydrate $CuSO_4·5H_2O$, *blue vitriol*, which has been recognized since antiquity.[1,2] Each year, thousands of high school ‡ and freshman college [3-5] students undertake 'copper cycle' laboratory experiments and wonder at the blue, gray and white materials that form as copper sulfate is heated and subsequently re-hydrated, but a good understanding of these observations is often lacking.§ While some advanced textbooks explain the structural changes,[6] no introductory texts that we could find explain the colour variation in copper sulfate hydrates using coordination chemistry concepts (Chart 1) although both coordination of aqua ions and the concept of crystal field theory is commonly included. Consequently, misconceptions on the cause of the colour changes are pervasive.§§ The focus of this paper is on *access to* the solid-state structures, many of which were originally determined a long time ago and are preserved in forms that make visualization and analysis challenging. Merely redetermining the structures on a modern X-ray diffractometer, and at low temperature as has become normative in current chemical practice is, however, not competitive to the best extant structures which employ neutron scattering. This limitation can now be addressed.

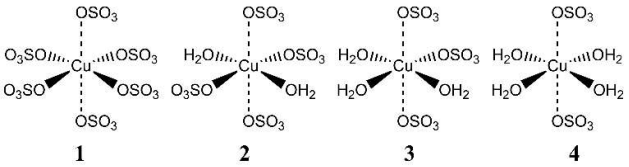

Chart 1 – Local coordination environments of the stable Cu(II) sulfates.

Copper(II) sulfate exists in four stable crystalline forms (Table 1): colourless anhydrous $CuSO_4$, **1** (mineral form: chalcocyanite);[7] the pale blue monohydrate $CuSO_4·H_2O$, **2** (mineral form: poitevinite);[8] the sky blue trihydrate $CuSO_4·3H_2O$, **3** (mineral form: bonattite);[9] and ubiquitous bright blue pentahydrate $CuSO_4·5H_2O$, **4** (mineral form: chalcanthite).[10] There is a significant *chemical* uniformity in these structures, (Chart 1) wherein the Cu^{2+} ion is always coordinated by four equatorial oxygen atoms in the d^9 *pseudo*-octahedral geometry with additional long axial bonds to oxygen.[11] The existing structural data are bookended by old but excellent structures for **1** (X-ray diffraction) [7] and **4** (single-crystal neutron diffraction),[10] but single crystal structures of **2** accessible in databases are without H positions and only a photographic X-ray diffraction determination of **3** has been reported which could not detect the H-atoms.[9] Rietveld powder neutron structures of these hydrates, generated to monitor *in situ* changes, have apparently not been deposited.[12]

There is still intensive interest in the copper sulfate system, which has been shown to hydrate and dehydrate in a series of distinct steps (on heating, **4** converts to **3** at ~80 °C; to **2** at ~120 °C, and to **1** above 240 °C).[12] The anhydrous powder is used as a laboratory desiccant and as an indicator in other drying agents

[a] *Department of Chemistry and Biochemistry, University of Lethbridge, Lethbridge, AB Canada.*
[b] *The Canadian Centre for Research in Advanced Fluorine Technologies (C-CRAFT), University of Lethbridge, Lethbridge, AB Canada.*

† Electronic Supplementary Information (ESI) available. Full electronic crystal models. CCDC 2119282; 2133582-2133584. For ESI and crystallographic data see DOI: 10.1039/x0xx00000x

Table 1 Crystal structures and mineral forms of copper(II) sulfate **1** and the stable hydrates **2** – **4**. [a]

Parameter	$CuSO_4$ (**1**) [b]	$CuSO_4 \cdot H_2O$ (**2**) [c]	$CuSO_4 \cdot 3H_2O$ (**3**) [d]	$CuSO_4 \cdot 5H_2O$ (**4**) [e]
Mineral	Chalcocyanite	Poitevinite	Bonattite	Chalcanthite
Space Group	*Pnma*	$P\overline{1}$	*Cc*	$P\overline{1}$
a /Å	8.3958 (6)	5.0281 (5)	5.5708 (2)	5.9676 (2)
b /Å	6.6760 (4)	5.1502 (5)	12.9751 (4)	6.0957 (2)
c /Å	4.8270 (3)	7.5607 (9)	7.3754 (2)	10.6366 (3)
α /°	90	108.592 (12)	90	77.224 (3)
β /°	90	108.382 (12)	96.450 (3)	82.387 (2)
γ /°	90	91.359 (10)	90	72.434 (3)
V / Å^3	270.56 (3)	174.41 (4)	529.73 (3)	358.85 (2)
Z, *Z'*	4, 0.5	2, 1	4, 1	2, 1
d_{calc}/g·cm^3	3.918	3.382	2.679	2.311
CCDC codes	2133582	2133583	2119282	2133584

[a] All results from this work. [b] Compare Ref 7. [c] Compare Ref. 8. [d] Compare Ref. 9. [e] Compare Ref 10.

such as silica gel.[13] The hydration/dehydration mechanism and energetics of copper sulfate remain of significant interest with recent reports from Raman and teraHerz spectroscopies [14,15] and older studies of differential thermal analysis from the decomposition of **4**.[16-18] Dehydration by shock waves has recently been investigated.[19] The crystal engineering associated with the self-organization of polyvalent metal sulfates has recently received a major retrospective analysis.[20] Hydration of **1** has been studied using powder neutron diffraction on samples in a controlled-humidity chamber.[12] There is ongoing interest in the structures of copper sulfate hydrates in the mineralogical literature,[21] where the properties of the copper sulfates are extensively discussed.[22] Most are secondary minerals, e.g. forming naturally from air oxidation of primary copper ores.[23] All four of these copper sulfate minerals have been thoroughly described from a mineralogical perspective, especially in the work of Canadian Frank C. Hawthorne.[24] Nevertheless, such descriptions are not very accessible to chemists and quite naturally focus on the bewildering complexity of mixed metal sulfates as found in many minerals.

There is also intense current interest in radically improving crystal structure refinement methods from X-ray diffraction as recognition dawns that data quality, even from modern home lab instruments, now routinely exceeds the capabilities of the traditional Independent Atom Model (IAM) that has been the standard-bearer of single-crystal structure refinement in chemistry and mineralogical laboratories since its introduction in 1915![25] One feature of the IAM is the standard employment of neutral atom scattering factors, which may not be appropriate to ionic crystal structures, such as the copper(II) sulfates described here. On the other hand, assuming a full +2 charge on copper, and distributing the negative charges amongst numerous oxygen atoms in the sulfato ligands has not proven successful.[26] A key deficiency of the IAM is that H nuclei are placed too close to the atoms they are bonded to – in strong contrast to diffraction by neutrons, which directly detect the nuclei and are especially sensitive to both the ^1_1H and ^2_1D isotopes.[27]

Fast and accurate density-functional theory (DFT) methods have become commonplace and make it entirely feasible to compute accurate, custom, atom scattering factors that directly reflect the electron densities of atoms *in their structural environment*, and thus polarized correctly to the precise location of each atom in a structure. This approach, one aspect of emerging quantum crystallography, remains a fully experimental structure determination because it uses DFT only to calculate atomic scattering factors. But calculated for the actual structure, rather than using standard compiled parameters from very old self-consistent field (SCF) calculations on a set of spherical, neutral atoms.[28]

With these custom scattering factors in hand, Hirshfeld Atom Refinement (HAR) can be implemented for the refinement of the atom position and displacement parameters.[29] A recent implementation of HAR in the program NoSpherA2,[30] incorporated into the popular structure determination package Olex2 v.1.5,[31] seamlessly integrates DFT from several popular computational packages with X-ray structure refinement using olex2.refine,[32] a powerful code that is comparable to, and compatible with, the trusted, reliable ShelXL method but implemented in modern programming languages in an open-source, extensible environment.

Herein we show that Hirshfeld atom refinement (HAR) using quantum crystallography affords accurate structures using conventional X-ray crystallography practices which can locate the hydrogen atoms (in the hydrates) with near neutron precision – at a much lower experimental cost. With the structures in hand, the dramatic loss of colour with reduced water content becomes much easier to understand and can be rationalized using simple crystal field theory applied to the strongly Jahn-Teller (J-T) distorted six-coordinate *pseudo*-octahedral geometries of the Cu(II) ions, consistent with their d^9 electron configurations.[11]

Results and discussion

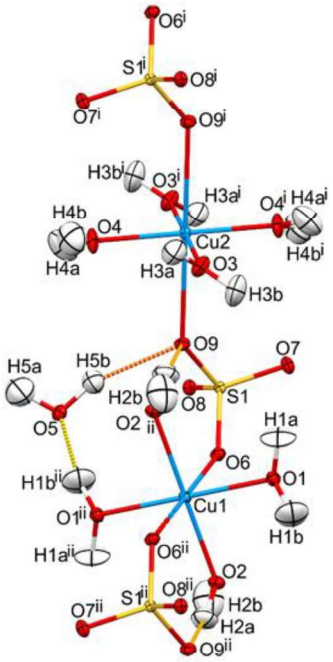

Figure 1. Displacement ellipsoids plot (50% probability) of the asymmetric unit in the crystal structure of **4** with atom numbering scheme, with expansion to show full coordination at the Cu(II) ions (symmetry operators: *i* 1-x,2-y,-z; *ii* 1-x,1-y,1-z).

Table 2 Key interatomic distances (Å) and angles (°) in the crystal structure of **4**.

Cu1-O1	1.9684 (8)	Cu1-O9	2.4100 (7)
Cu1-O2	1.9757 (7)	S1-O6	1.4751 (7)
Cu1- O6	2.3618 (7)	S1-O7	1.4759 (8)
Cu1-O7	1.9615 (16)	S1-O8	1.4910 (7)
Cu2-O3	1.9673 (7)	S1-O9	1.4783 (7)
Cu1-O4	1.9355 (8)		
O1-Cu1-O2	88.30 (3)	O3-Cu2 O4	89.60 (3)
O1-Cu1-O2^{ii}	91.70 (3)	O3-Cu2-O4^{i}	90.40 (3)
O1-Cu1-O6	92.18 (3)	O3-Cu2-O9	91.97 (3)
O2-Cu1-O6	87.73 (3)	O4-Cu2-O9	93.35 (3)
Cu1-O6-S1	132.10 (4)	O6-S1-O9	109.46 (4)
Cu2-O9-S1	138.37 (4)	O7-S1-O8	108.83 (4)

^{i} *+x,2-y,-z*, ^{ii} 1-*x*,1-*y*,1-*z*

Structure and Hirshfeld Atom refinement of $CuSO_4·5H_2O$, 4

The detailed structure descriptions are introduced in 'reverse order' by starting with the pentahydrate since it is by far the most familiar to most chemists. In **4** (Fig. 1 and Table 2), there are two crystallographically independent Cu(II) ions, each located at a $\overline{1}$ symmetry site with half-occupancy, and coordinated by four water molecules in the equatorial planes (Cu1, O1, O2 and Cu2, O3, O4) with short bonds (1.9355 (4) - 1.9757 (7) Å), complemented by sulfate O donors in the J-T elongated axial sites (O6 and O9) with long bonds (2.3618(7) and 2.4100(7) Å). These values are in excellent agreement with 1.94 Å to equatorial and 2.38 Å to axial water oxygen atoms found by Ohtaki in aqueous Cu(II) sulfate from X-ray scattering probability distribution curves [33] (or conc. dependent 1.97 Å equatorial and 2.34 – 2.39 axial in another study by Magini).[34] The average ratio of axial to equatorial lengths is 1.22:1, comfortably within the two sets of ratios from the Ohtaki [33] and Magini studies.[34] This reinforces the notion that in structure **4**, aqua copper has crystallized retaining the four strongly-bound equatorial water molecules in $[Cu(OH_2)_6]^{2+}$ but replacing the weakly bound axial waters by sulfate oxygens. Crystal structures retaining the hexahydrate are rare, found e.g. in the Tutton salt, $[NH_4]_2[Cu(OH_2)_6][SO_4]_2$.[35]

There is only one independent sulfate anion, located at a general position in $P\overline{1}$, which bridges Cu1 and Cu2 through O6 and O9, whereas O7 and O8 are only involved in hydrogen bonding. Both terminal and coordinated sulfate O atoms form H-bonds and the fifth water molecule (O5) is hydrogen bonded (as acceptor) to coordinated water H1b and (as donor) to sulfate O9. This new X-ray diffraction refinement is in good agreement with the excellent parallel single crystal neutron diffraction studies on $CuSO_4·5H_2O$ and $CuSO_4·5D_2O$ of Bacon.[10] Interatomic distances and angles in our structure determination are strongly comparable to the earlier neutron study, except that Cu–O distances are 0.54 % shorter, which we attribute to the ~200 K lower crystal temperature in our measurements. For further details on H-bonding, see below.

Structure and Hirshfeld Atom refinement of $CuSO_4·3H_2O$, 3

The original X-ray crystal structure report on **3** by Zahrobsky and Baur,[9] using photographic methods at ambient temperature with Mo *K*α radiation, is essentially correct but was not able to locate hydrogen atoms directly, crucial to an accurate delineation of the H-bonding network that is of central importance to the lattice structure of hydrated metal salts.[38-40] To the best of our knowledge, only one redetermination of this structure has been reported in the literature, which is from a Rietveld refinement of powder neutron diffraction data on a mixture obtained by gradual hydration of powdered **1**, also at ambient temperature.[12] This refinement does not seem to have been deposited in any crystallographic database. Here we report a modern, low-temperature single-crystal structure determination at 100 K on a synthetic sample of **3** where all six water H-atoms could be located on a difference map and were refined anisotropically.

A quality single crystal of **3** was originally made accidentally by oxidation of CuCl with SO_2Cl_2, followed by hydrolysis in acetonitrile and evaporation in low-humidity air. Even better crystals were obtained from slow cooling of a warm solution composed of a 8:55:37 weight-% ratio of $CuSO_4·5H_2O$/ H_2SO_4/H_2O.[41] A hemisphere of data was collected so as to have sufficient Friedel pairs to refine the correct handedness of the unit cell in the chiral space group *Cc* and to increase redundancy. Depictions of the resulting structure are found in Fig. 2, key interatomic distances and angles in Table 3, and H-bonding data in Table 6. The structure in space group *Cc* has no site symmetry and the asymmetric unit corresponds to the equatorial plane of coordination (atom labels without superscripts in Fig. 2).

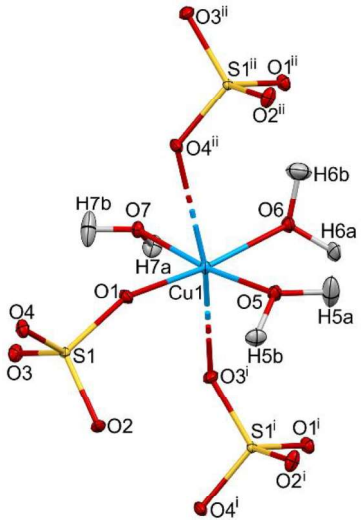

Figure 2. Displacement ellipsoids plot (50% probability) of the asymmetric unit in the crystal structure of **3** with atom numbering scheme. Symmetry equivalent sulfates (symmetry operators: [i] +*x*,1-*y*,-1/2+*z*, [ii] +*x*,1-*y*,-1/2+*z*) are included to complete the axial ligation.

In structure **3**, Cu---O–S coordination in the equatorial plane occurs exclusively to O1 of the sulfate ion, while O3 and O4 (in symmetry-related SO_4^{2-} ions) coordinate as axially-elongated donors to Cu(II), while O2 is not bonded to Cu but instead only forms H-bonds. Interestingly, three sulfate oxygen atoms in the structure are tricoordinate; for O1 this involves S, Cu and H6b, for O3, S, Cu and H6a, for O2 it is S and two H-bonds, to H7A and H7B (Table 6). By contrast, four coordinate O4 bridges to Cu as well as forming H-bonds to H5A and (weaker) to H6B. Only one of the three coordinated water molecules is linked to a second coordinated H_2O via H-bonding, namely H5B to O7[ii]. O1 which, consistent with its equatorial position, forms the shortest sulfate ion bond to Cu, also has the longest S–O bond at 1.4943 (10) Å, about 1.5% longer than the average of 1.4726 (12) Å for the three other S–O bonds in each sulfate ion, which is statistically significant in this refinement at the 99 % confidence level.[42]

At the metal, the four equatorial Cu–O bond lengths are indistinguishable at the 99% confidence level and average to 1.9641 (10) Å, with no apparent distinction between water and sulfate O donors. This value is in good agreement with 1.94-1.97 Å for the equatorial water ligands in aqueous Cu(II) sulfate from X-ray scattering probability distribution curves.[33,34] In strong contrast, the two axial bonds are distinctly longer and different from each other at 2.3726 (10) and 2.4460 (10) Å. The shorter of these distances, to O3[i], is 21% longer than the equatorial average, and matches well to 2.34-2.39 Å for axial waters in solution.[33,34] The second distance to O4[ii] is 25% longer, exceeds this and hence likely exceeds the intrinsic bond lengthening expected from Jahn-Teller distortions.[11] Lattice effects and the competition between coordination and H-bonding energies likely accounts for this variation. An indication that these lattice forces have a considerable impact is the large difference

Table 3 Key interatomic distances (Å) and angles (°) in the crystal structure of **3**.

Cu1-O1	1.9571 (9)	Cu1-O3[i]	2.3726 (10)
Cu1-O5	1.9559 (9)	S1-O1	1.4943 (10)
Cu1- O6	1.9817 (11)	S1-O2	1.4716 (10)
Cu1-O7	1.9615 (9)	S1-O3	1.4719 (10)
Cu1-O4[ii]	2.4460 (10)	S1-O4	1.4742 (10)
O1-Cu1-O4[ii]	101.38 (6)	O1-Cu1 O3[i]	80.25 (6)
O1-Cu1-O6	171.08(8)	O7-Cu1-O3[i]	81.03 (7)
O5-Cu1-O1	85.72(11)	O3[i]-Cu1-O4[ii]	165.63 (6)
O5-Cu1-O4[ii]	101.38 (6)	Cu1-O1-S1	141.56 (12)
O5-Cu1-O6	90.89 (8)	Cu1-O4[ii]-S1[ii]	139.26 (10)
O5-Cu1-O7	173.45 (7)	Cu1-O3[i]-S1[i]	128.35 (9)
O6-Cu1-O4[ii]	88.77 (6)	O2-S1-O1	108.90 (11)
O7-Cu1-O1	95.64 (8)	O2-S1-O3	110.87 (15)
O7-Cu1-O4[ii]	84.65 (6)	O3-S1-O1	106.15 (10)
O7-Cu1-O6	86.67 (8)	O4-S1-O1	110.29 (10)
O6-Cu1-O3[i]	91.64 (7)	O4-S1-O2	110.43 (9)
O5-Cu1-O3[i]	92.98 (6)	O4-S1-O3	110.11 (10)

[i] +*x*,1-*y*,-1/2+*z*, [ii] +*x*,1-*y*,-1/2+*z*

between the acute equatorial O–Cu–O angles, which average to 86.36 (6)°, and those involving the axial sites, which range from a low of 80.29 (4) to high of 88.79 (4)°. The *overall* distortion from a regular octahedron in **3** is higher than in anhydrous **1**, although the single largest deviation is found in the latter. In summary, the Cu–O distances in the lattice remain close to the values for $[Cu(OH_2)_6]^{2+}$ in water whereas the angles deviate up to 10° from the expected right angles.

Structure and Hirshfeld Atom refinement of $CuSO_4 \cdot H_2O$, 2

In monohydrated **2** (Fig. 3 and Table 4), there are again two independent Cu(II) ions located at $\overline{1}$ symmetry sites with half-occupancy as in the structure of **4**, but here coordinated twice by water oxygen and four times by sulfate O atoms. The unique water molecule bridges the two copper ions through O1, and the unique sulfate bridges the same pair of Cu ions via the O2 and O3 atoms, forming an asymmetrical six-membered Cu1-O1-Cu2-O3-S1-O2 ring. Two proximate Cu1 ions are bridged by two sulfates via O2 and O5 in an eight-membered ring. Further bridging rings are formed by H-bonds between sulfate O atoms and the two water H-atoms. Unique to **2** is that Cu1 has two short equatorial bonds to water O atoms (2.018 (6) Å) and to sulfate O2 (1.967 (6) Å), with two much longer axial bonds to sulfate O5 (2.289 (6) Å), whereas Cu2 has four shorter equatorial bonds to sulfates {O3 1.946 (6) and O4 1.971 (6) Å} but the *long* axial bonds are both to water {2.422 (7) Å}. Since the aqua oxygen exerts the larger crystal field, this structural anomaly contributes to the paleness of the colour of **2** (see below). The average ratio of axial to equatorial lengths is 1.19:1, and hence smaller than the ratios found for aqua Cu(II) in solution,[33,34] suggesting that the J-T distortion for sulfato ligands is somewhat lower than that for aqua ligands.

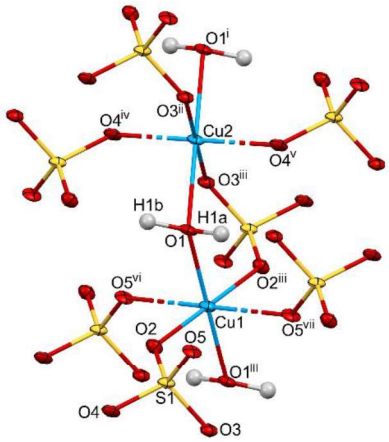

Figure 3. Displacement ellipsoids plot (50% probability) of the asymmetric unit in the crystal structure of **2** with atom numbering scheme. Expansion to show full coordination at the Cu(II) ions (symmetry operators: *i* -x,-y,-z; *ii* -1+x,-1+y,-1+z; *iii* 1-x,1-y,1-z; *iv* -x,1-y,1-z; *v* x,-1+y,-1+z; *vi* x,-1+y,z; *vii* 1-x,2-y,1-z).

Table 4 Key interatomic distances (Å) and angles (°) in the crystal structure of **2**.

Cu1-O1	2.018 (6)	Cu2-O4^{iii}	1.971 (6)
Cu1-O2	1.967 (6)	S1-O2	1.472 (7)
Cu1-O5^{i}	2.289 (6)	S1-O3	1.499 (7)
Cu2-O1	2.422 (7)	S1-O4	1.476 (7)
Cu2-O3^{ii}	1.946 (6)	S1-O5	1.450 (6)
O1-Cu1-O2	89.0 (3)	Cu2^{ii}-O3-S1	131.6 (4)
O1-Cu1-O5^{iv}	89.1 (2)	Cu2^{vii}-O4-S1	136.3 (4)
O2-Cu1-O5^{iv}	82.5 (3)	O2-S1-O3	109.1 (4)
O1-Cu2-O3^{i}	88.6 (2)	O2-S1-O4	108.2 (4)
O1-Cu2-O4^{v}	83.0 (2)	O3-S1-O4	108.8 (4)
O3^{i}-Cu2-O4^{v}	85.5 (3)	O2-S1-O5	112.1 (4)
Cu1-O1-Cu2	119.4 (3)	O3-S1-O5	108.8 (4)
Cu1-O2-S1	130.9 (4)	O4-S1-O5	110.9 (4)
Cu1^{vi}-O5-S1	134.7 (4)		

^{i} -1+*x*,-1+*y*,-1+*z*, ^{ii} 1-*x*,1-*y*,1-*z*, ^{iii} -*x*,1-*y*,1-*z*, ^{iv} +*x*,-1+*y*,+*z*, ^{v} +*x*,-1+*y*,-1+*z*, ^{vi} +*x*,1+*y*,+*z*, ^{vii} +*x*,1+*y*,1+*z*.

Structure and Hirshfeld Atom refinement of anhydrous $CuSO_4$, 1

In anhydrous **1** (Fig. 4 and Table 5) in space group *Pmna*, the Cu(II) ion is located at a special position with $\bar{1}$ symmetry, but the unique sulfate ion is located on the *m* plane through S, O1 and O2, so that the whole formula unit has half-occupancy (*Z'* = 0.5, Table 1). All coordination is therefore from sulfate O atoms, with the usual distinction between four short equatorial (O2, O3) and two much longer axial bonds (O1), consistent with the J-T distortion of this d^9 metal ion. The Cu-O2 bonds are 2.0433 (7), the Cu-O3 1.9194 (8) and the Cu-O1 2.3618 (8) Å. The average ratio of axial to equatorial lengths is 1.19:1, the same as found in **2**, and hence smaller than the ratios found for aqua Cu(II) in solution,[33,34] lending further weight to the notion that the J-T distortion for sulfato ligands is somewhat lower than that for aqua ligands.

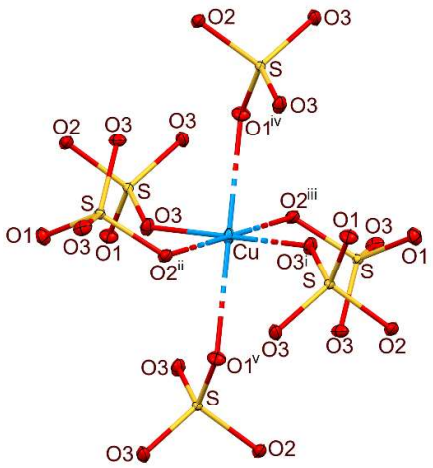

Figure 4. Displacement ellipsoids plot (50% probability) of the asymmetric unit in the crystal structure of **4** with atom numbering scheme. Expansion to show full coordination at one Cu(II) ion (symmetry operators: i -x,-y,-z ; ii 1/2-x,-y,-1/2+z; iii -1/2+x,1/2-y,1/2-z ; iv x,y,-1+z; v -x,-1/2+y,1-z).

Table 5 Key interatomic distances (Å) and angles (°) in the crystal structure of **1**.

Cu-O1^{i}	2.3618 (8)	S-O3	1.4645 (8)
Cu-O2^{ii}	2.0433 (7)	O1-S-O2	110.31 (7)
Cu- O3	1.9194 (8)	O1-S-O3	110.52 (4)
O1^{i}-Cu-O2^{ii}	103.87 (3)	O2-S-O3	105.96 (4)
O1^{i}-Cu-O2^{iii}	76.13 (3)	O3-S-O3^{iv}	113.36 (7)
O1^{i}-Cu-O3	90.84 (4)	Cu-O1^{i}-Cu^{i}	89.93 (4)
O1^{ii}-Cu-O3	89.16 (4)	Cu-O2^{ii}-Cu^{ii}	109.53 (5)
O2^{ii}-Cu-O3	91.05 (4)	S-O1-Cu^{v}	130.57 (3)
O2^{iii}-Cu-O3	88.95 (4)	S-O2-Cu^{iii}	123.44 (3)
S-O1	1.4563 (12)	S-O3-Cu	136.63 (5)
S-O2	1.5170 (12)		

^{i} -*x*,-1/2+*y*,1-*z*, ^{ii} -1/2+*x*,1/2-*y*,1/2-*z*, ^{iii} 1/2-*x*,-*y*,-1/2+*z*, ^{iv} +*x*,1/2-*y*,+*z*, ^{v} -*x*,1/2+*y*,1-*z*.

Hydrogen bonding in structures 4, 3 and 2

In fully hydrated **4** both terminal and coordinated sulfate O atoms form H-bonds and the fifth water molecule (O5) donates to coordinated sulfate O6 and O9 on two different Cu complexes and accepts from coordinated waters H1B and H2B on two further Cu complexes so that it is fully ensconced in H-bonds, reminiscent of water in ice crystals (Table 6 and Fig. 5d). All four symmetry inequivalent water ligands H-bond through both H atoms; in all, ten (relatively strong) electrostatic-covalent H-bonds [38-40] and two weaker ones have been calculated. There is also excellent correlation in the H-atom positions and O–H bond lengths compared to the 1975 ambient temperature neutron diffraction report, after allowance is made for contraction at 100 K (the italic entries in each second row of Table 6).[10] This demonstrates the ability of HAR with NoSpherA2 to accurately determine the true positions of H-atoms via single crystal X-ray diffraction.

ARTICLE

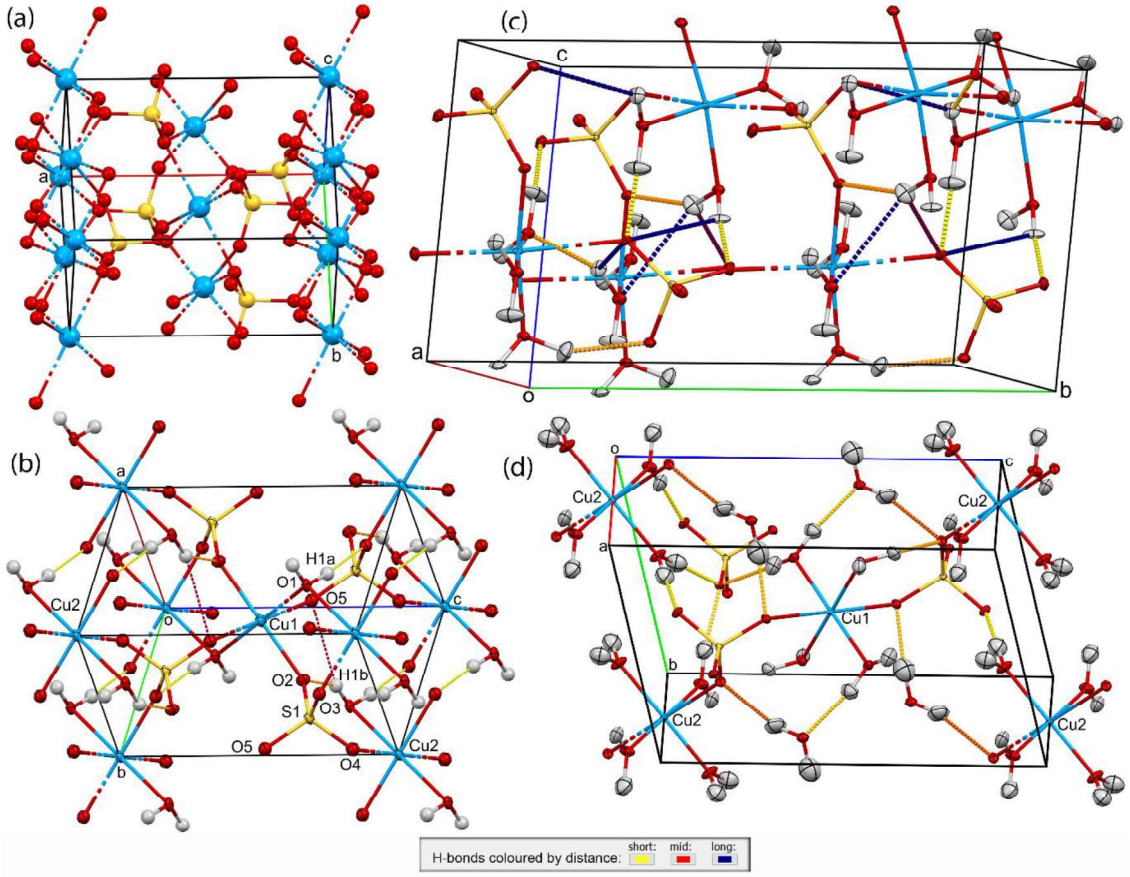

Figure 5. Unit cell packing diagrams of (a) $CuSO_4$ **1**, (b) $CuSO_4{\cdot}H_2O$ **2**, (c) $CuSO_4{\cdot}3H_2O$ **3** and (d) $CuSO_4{\cdot}5H_2O$ **4**. Displacement ellipsoids plots are drawn at 50% probability in (b) – (d) whereas (a) is clearer as a *ball and stick* representation; H atoms in **3** are isotropic, also at 50% probability. The intermolecular H-bonds in **2** – **4** are shown as dashed lines coloured by distance as per the legend at bottom.

In the original RT X-ray diffraction structure of $CuSO_4{\cdot}3H_2O$, **3**, obtained by precession photography in 1968,[9] the H atoms were calculated by assuming positions of least electrostatic energy, and the water molecules are all placed axially coordinated to the Cu centre. On this basis, it was concluded that only four of six unique H atoms are involved in H-bonding. Satisfyingly, with the more accurate placement resulting from our NoSpherA2 refinement, all six H-atoms can clearly be shown to be involved in (relatively strong) conventional electrostatic-covalent H-bonding (Table 6 and Fig. 5c).[38-40]

By contrast, the Rietveld powder X-ray diffraction of Ting *et al*. in 2009, while also conducted at ambient temperature, was able to place H atoms experimentally, as expected with neutron data.[12] However, these authors commented on the large variability in the U_{eq} measured for different H atoms and make the claim that stronger H-bonding would lead to more localized atom positions. There is a very good match in the *positions* of H atoms between our X-ray structure and that of Ting *et al.* but our refinement shows much greater uniformity in *displacements*, as is evident from the U_{eq} data from the two datasets in Table 6 and from Figs. 2 and 5c.[12] A comparison of the structural data suggests that the HAR gives better accuracy in H-atom placement and displacement than this *powder* Rietveld determination, whereas the combined protonated/deuterated single crystal neutron diffraction structure of $CuSO_4{\cdot}H_2O$ is competitive with that of **4** although heavy atom bond precision is better in our structure at 100 K.[10]

Table 6. Hydrogen bonding parameters in **2 - 4** compared with single-crystal and powder neutron diffraction data (in following rows, *Italic*, where avail.)

D-H···A	d(D-H)/Å	d(H-A)/Å	d(D-A)/Å	D-H-A/°	Ueq
4 [a]					
O4-H4A···O7^{i}	0.947 (14)	1.720 (15)	2.6653 (11)	175.7 (19)	0.029 (5)
	0.968(6)	*1.712(6)*	*2.678(4)*	*176.0(3)*	*0.035 (2)*
O4-H4B···O8^{i}	0.961 (14)	1.752 (15)	2.6930 (10)	166 (2)	0.029 (5)
	0.963(5)	*1.761(5)*	*2.707(5)*	*167.0(5)*	*0.035 (2)*
O3-H3A···O7	0.964 (14)	1.754 (14)	2.7017 (11)	166.7 (17)	0.024 (5)
	0.971(5)	*1.747(4)*	*2.715(4)*	*174.7(4)*	*0.35 (2)*
O2-H2B···O5^{ii}	0.947 (13)	1.781 (13)	2.7271 (11)	176.2 (17)	0.027 (5)
	0.982(5)	*1.771(5)*	*2.747(5)*	*172.0(6)*	*0.035 (2)*
O3-H3B···O8^{iii}	0.969 (14)	1.791 (14)	2.7424 (11)	166.5 (18)	0.027 (5)
	0.960(5)	*1.807(5)*	*2.756(4)*	*169.3(5)*	*0.035 (2)*
O1-H1B···O5^{iv}	0.950 (13)	1.812 (14)	2.7494 (11)	168.4 (18)	0.021 (5)
	0.960(5)	*1.834(7)*	*2.781(5)*	*168.3(6)*	*0.035 (2)*
O5-H5A···O6^{v}	0.964 (15)	1.810 (15)	2.7601 (11)	167.6 (19)	0.042 (6)
	0.978(5)	*1.820(5)*	*2.784(4)*	*168.1(4)*	*0.035 (2)*
O2-H2A···O9^{vi}	0.971 (14)	1.895 (16)	2.7855 (10)	151.3 (17)	0.019 (5)
	0.971(8)	*1.893(7)*	*2.795(5)*	*153.5(5)*	*0.035 (2)*
O1-H1A···O8^{vii}	0.962 (14)	1.875 (15)	2.8113 (11)	163.5 (17)	0.025 (5)
	0.961(6)	*1.913(7)*	*2.854(5)*	*165.6{5)*	*0.035 (2)*
O5-H5B···O9^{v}	0.963 (15)	2.015 (16)	2.9388 (11)	160.0 (19)	0.042 (6)
	0.936(11)	*2.084(10)*	*2.985(6)*	*161.4(5)*	*0.035 (2)*
O2-H2A···O3^{viii}	0.971 (14)	2.517 (18)	3.1423 (11)	122.1 (14)	0.019 (5)
O1-H1A···O6^{iii}	0.962 (14)	2.494 (17)	3.1997 (11)	130.1 (14)	0.025 (5)
3 [b]					
O7-H7A···O2^{ix}	1.000 (15)	1.621 (16)	2.6022 (13)	166 (2)	0.013 (5)
	0.99	*1.63*	*2.618*	*176*	*0.02*
O7-H7B···O2^{x}	0.954 (16)	1.78 (2)	2.6667 (13)	153 (3)	0.024 (5)
	0.98	*1.69*	*2.655*	*166*	*0.06*
O5-H5A···O3^{ix}	0.998(15)	1.687 (16)	2.6841 (13)	178 (3)	0.023 (6)
	0.98	*1.58*	*2.509*	*157*	*0.04*
O6-H6A···O4^{xi}	0.978 (15)	1.776 (16)	2.7505 (14)	174 (2)	0.013 (5)
	0.98	*1.83*	*2.761*	*158*	*0.04*
O5-H5B···O7^{xii}	1.001 (15)	1.890 (19)	2.8141 (13)	152 (2)	0.012 (5)
	0.98	*1.87*	*2.821*	*162*	*0.03*
O6-H6B···O1^{xiii}	0.993 (16)	1.94 (2)	2.8448 (15)	151 (2)	0.018 (5)
	0.98	*1.91*	*2.831*	*156*	*0.06*
O6-H6B···O4^{xiv}	0.993 (16)	2.48 (2)	3.1589 (15)	125 (2)	0.018 (5)
2 [b]					
O1-H1A···O3^{xv}	0.992 (19)	1.70 (3)	2.692 (9)	173 (14)	0.0155 (16)
	0.972	*1.851*	*2.819*		*0.0150(4)*
O1-H1B···O2^{xvi}	0.992 (19)	1.91 (9)	2.808 (9)	150 (14)	0.0155 (16)
	0.988	*2.017*	*2.717*		*0.12(1)*
O1-H1B···O5^{xvii}	0.992 (19)	2.38 (13)	3.088 (9)	128 (12)	0.0155 (16)
	0.988	*2.153*	*3.012*		*0.12(1)*

[a]Data in italics are from the 1975 single crystal neutron structure.[10] The U_{eq} values are taken from the 2009 Rietveld powder neutron structure.[12] [b]Data in italics are from the 2009 Rietveld powder neutron structure. No s.u. were reported in the neutron study, which does not appear to have been deposited.[12] (Symmetry operators: ^{i}-1+x,+y,+z; ^{ii}+x,-1+y,1+z; ^{iii}1-x,1-y,1-z; ^{iv}1+x,+y,+z; ^{v}2-x,1-y,-z; ^{vi}2-x,2-y,-z; ^{vii}1-x,1-y,-z; ^{viii}1-x,-y,1-z; ^{ix}+x,+y,-1+z; ^{x}1+x,+y,+z; ^{xi}-1/2+x,3/2-y,-1/2+z; ^{xii}-1+x,+y,-1+z; ^{xiii}-1+x,1-y,-1/2+z; ^{xiv}-1+x,+y,+z ; ^{xv} 1-x,1-y,1-z, ^{xvi} -x,1-y,1-z, ^{xvii} -x,1-y,1-z.)

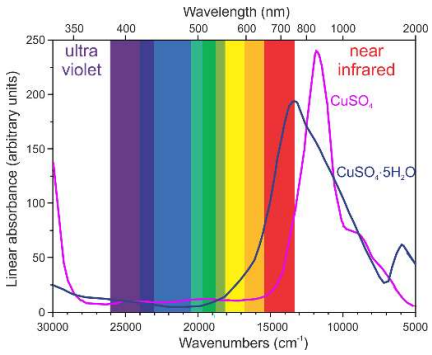

Figure 6. Solid-state electronic absorption spectra of (blue line) chalcanthite and (pink line) chalcocyanite superimposed on the approximate wavenumber regions of light. Adapted, with permission, from Springer: M. Wildner, G. Giester, M. Kersten. K. Langer, *Phys. Chem. Minerals*, 2014, **41**, 669, and Mineralogical Society of America: G. J. Redhammer, L. Koll, M. Bernroider, G. Tippelt, G. Amthauer and G. Roth, *Amer. Mineral.* 2007, **92**, 532.

In **2**, the sulfate ions are all fully coordinated to copper and the water oxygen atom O1 bridges two metal centres. Both H1A and H1B form (relatively strong) conventional H-bonds to, in all, three symmetry-related sulfates through O2, O3 and O5 (Table 6, Fig. 5b).[8] A consideration of the unit cell packing diagrams (Fig. 5a,b) suggests that the water of hydration in **2** has inserted into two of the Cu-OSO_3 bonds of the anhydrous lattice of **1**. Note also that with each stage of hydration, the density of the resultant lattice is stepwise reduced (Table 1). The anhydrous crystal is thus very compact and rigid, although the angle strain to the axial ligands is presumably high (e.g. O1^{i}-Cu-O2^{iii} = 76.13 (3)° (Table 5).

Why does the colour change with degree of hydration?

$[Cu(OH_2)_6]^{2+}$ in dilute solution is blue due to exclusive absorption of red wavelengths of light, but the band maximum is in the near IR (13 000 cm^{-1}). The band maximum in solid chalcanthite at 13 308 cm^{-1} (Fig. 6) is clearly very similar to aqua Cu(II).[43] In a tour de force investigation, Wildner and colleagues have reported a detailed polarized electronic absorption spectrophotometry study of crystalline anhydrous $CuSO_4$, in part to address "the perplexing absence of colour of chalcocyanite, $CuSO_4$".[44] Their spectra demonstrate that the band maximum shifts to 11 720 cm^{-1} and that the band profile has a steep rise to this peak, followed by further shoulders at lower energies. The result is that crystalline chalcocyanite absorbs virtually no red light (Fig. 6). Moreover, the high-energy bands not involving *d-d* transitions have thresholds above 27 000 cm^{-1}, comfortably within the UV spectral region. Consequently, $CuSO_4$ is virtually transparent to visible light, and hence almost colourless.

The tetragonally elongated structures (see above) have effective D_{4h} symmetry (4 + 2 coordination) and Redmann *et al*. have shown that the E_g level is strongly split, approximating to that of a square planar geometry.[43] The highest energy *d-d* transition, $^{2}Eg \rightarrow {}^{2}B_{1g}$, is therefore dominated by the crystal fields of the equatorial ligands. In **1** all four of these are sulfato oxygen donors, whereas in **3** there are one sulfato and three water O donors, and in **4** all four donors are water (hence the

similarity of the optical spectrum of **4** and aqua $[Cu(OH_2)_6]^{2+}$ is not surprising). Structure **2** is a special case as only half the Cu(II) sites have two equatorial water ligands and the other half are all sulfato – so there are on average one water and three sulfato equatorial ligands.

Simply put, the crystal field splitting by H_2O is greater than by SO_4^{2-}.[45] A compounding factor *for colour* is that the band profile of the anhydrate is much narrower than that of the pentahydrate. This is probably attributable to the more rigid structure (reflected in the 1.7X higher density). We can expect the H-bonded networks of the hydrates to have greater elasticity, with more facile Cu–O vibrations increasing the absorption bandwidths.[11] Progressive increase in hydration therefore shifts the absorption bands to higher energies, into the lowest energy visible region (red light) and hence hydrated and partly hydrated Cu(II) salts, and the aqua ions in solution, appear with different shades of blue.

Experimental

Sample sources

$CuSO_4{\cdot}5H_2O$ (Fisher, technical grade) was recrystallized from a saturated aqueous solution to afford bright blue trapezoidal plates. The recrystallized material was used for all subsequent work. Several very small lozenge-shaped crystals also formed, which were used to obtain the crystal structure of **4**, after carefully splitting these crystals multiple times to obtain a sufficiently small crystal. Buffering the crystals from shock within the Paratone® crystal mounting oil was essential to the cleaving process. CAUTION: *98% H_2SO_4 is a strong desiccant as well as strong acid. Wear appropriate gloves and eye protection; conducting work in an adequate fume hood is strongly advised.*

Crystals of $CuSO_4{\cdot}1H_2O$ **2** and $CuSO_4{\cdot}3H_2O$ **3** were obtained using an understanding of the $CuO/SO_3/H_2O$ phase diagram [23] following the method reported by Götz.[41] 0.80 g of $CuSO_4{\cdot}5H_2O$ (8 wt.%) was dissolved in 3.7 g H_2O (37 wt.%) in a 20 mL Erlenmeyer flask and gently heated on a hot plate. To this was carefully added 5.5 g of 98% H_2SO_4 (55 wt.%) so as not to boil the solution. The resulting pale blue solution was cooled slowly overnight by turning off the hot plate. In the morning, clumps of sky-blue crystals had formed, which were filtered off on a coarse fritted glass funnel, 0.27 g (34% yield). The smallest clumps were transferred to Paratone® crystal mounting oil where they presented as aggregated blocks of almost colourless crystals that could be separated with a razor blade to afford bona fide single crystals in the oil. One of these crystals was mounted on the diffractometer and identified as **3**.

The mother liquor from the synthesis of **3** described above was gently boiled on the hot plate for 3 H and concentrated to about ¾ the original volume. On cooling overnight, clusters of palest blue crystals of **2** formed at the bottom, filtered on the fritted funnel, transferred to a microscope slide and immersed in Paratone®. The crystals were readily identified as **2** from the unit cell parameters, but crystal quality was poor with excessively high R_{int} on intensities. Careful searching resulted in the identification of very small flat needles. These crystals were adequate but still not of excellent diffraction quality. The smallest crystals, requiring the brighter Cu Kα source, gave the best results and one of these was used for the reported structure.

Crystals of anhydrous $CuSO_4$ **1** were obtained following the method of Gruzensky.[46] 2.64 g $(NH_4)_2SO_4$ was dissolved by heating with an open flame in 7.84 g of 98% H_2SO_4 contained in a 20 mL borosilicate test tube (TT) and the mixture boiled for several minutes. Finely ground $CuSO_4{\cdot}5H_2O$ was dehydrated in an oven at 130 °C for 3 H until grey/white in colour and added to the 20/80 mole fraction mixture until saturated at the boil. Slow cooling of the faintly blue solution was achieved by placing the end of the TT on a hot plate for several hours. Thereafter the heating was stopped, and the TT left undisturbed overnight. A fine precipitate of colourless crystals was obtained of which a portion were transferred to Paratone® crystal mounting oil. Suitable uniformly shaped prisms were selected under the microscope, mounted, and identified as **1** by the unit cell parameters. Data was collected using Mo Kα radiation at 100 K.

Crystallography

Crystals were mounted on the diffractometer using a 100 µm MiTeGen loop and kept at 100.00 (10) K during data collection. Data collection and data processing were under the control of CrysAlisPro release 1.171.41.116a (Rigaku Oxford Diffraction, 2021). Using Olex2,[31] the structures were solved with the ShelXT [47] structure solution program using Intrinsic Phasing and refined with the olex2.refine [32] refinement package using Levenberg-Marquardt minimization. Data analysis was performed and illustrations prepared with Mercury CSD 2021.2.[48]

Crystal and experimental data for 1. CuO_4S (M =159.609 g/mol): orthorhombic, space group *Pnma* (no. 62), a = 8.3958 (6) Å, b = 6.6760(4) Å, c = 4.8270 (3) Å, V = 270.56 (3) Å^3, Z = 4, T = 100.0 (3) K, µ(Mo Kα) = 8.637 mm^{-1}, D_{calc} = 3.918 g/cm^3, 3682 reflections measured (9.72° ≤ 2Θ ≤ 76.18°), 738 unique (R_{int} = 0.0344, R_{sigma} = 0.0251) which were used in all calculations. The final R_1 was 0.0205 (I≥2σ(I)) and wR_2 was 0.0535 (all data).

Crystal and experimental data for 2. CuH_2O_5S (M =177.625 g/mol): triclinic, space group $P\overline{1}$ (no. 2), a = 5.0281 (5) Å, b = 5.1502 (5) Å, c = 7.5607 (9) Å, α = 108.592 (12)°, β = 108.382 (12)°, γ = 91.359 (10)°, V = 174.41 (4) Å^3, Z = 2, T = 100.01 (10) K, µ(Cu Kα) = 13.717 mm^{-1}, D_{calc} = 3.382 g/cm^3, 3078 reflections measured (13.14° ≤ 2Θ ≤ 160.66°), 751 unique (R_{int} = 0.0399, R_{sigma} = 0.0243) which were used in all calculations. The final R_1 was 0.0746 (I≥2σ(I)) and wR_2 was 0.2140 (all data).

Crystal and experimental data for 3. CuH_6O_7S (M =213.655 g/mol): monoclinic, space group *Cc* (no. 9), a = 5.5708 (2) Å, b = 12.9751 (4) Å, c = 7.3754 (2) Å, β = 96.450 (3)°, V = 529.73 (3) Å^3, Z = 4, T = 100.01 (10) K, µ(Mo Kα) = 4.488 mm^{-1}, D_{calc} = 2.679 g/cm^3, 13522 reflections measured (6.28° ≤ 2Θ ≤ 76.32°), 2761 unique (R_{int} = 0.0375, R_{sigma} = 0.0284) which were used in all calculations. The final R_1 was 0.0188 (I≥2σ(I)) and wR_2 was 0.0428 (all data).

Crystal and experimental data for 4. $CuH_{10}O_9S$ (M =249.686 g/mol): triclinic, space group $P\overline{1}$ (no. 2), a = 5.9676 (2) Å, b = 6.0957 (2) Å, c = 10.6366 (3) Å, α = 77.224 (3)°, β = 82.387 (2)°, γ = 72.434 (3)°, V =

358.85 (2) Å^3, Z = 2, T = 100.00 (10) K, μ(Mo Kα) = 3.350 mm^{-1}, D_{calc} = 2.311 g/cm^3, 18712 reflections measured (7.14° ≤ 2Θ ≤ 76.6°), 3729 unique (R_{int} = 0.0463, R_{sigma} = 0.0349) which were used in all calculations. The final R_1 was 0.0249 (I≥2σ(I)) and wR_2 was 0.0512 (all data).

The refinements employed NoSpherA2,[30] (NOn-SPHERical Atom-form-factors in Olex2),[31] an implementation of HAR that makes use of tailor-made aspherical atomic form factors calculated on-the-fly from a Hirshfeld-partitioned electron density (ED). The ED is calculated from a Gaussian basis set single determinant SCF wavefunction in DFT at the B3LYP/def2-SVP (**1**, **4**), B3LYP/6-31G(d,p) (**2**), and PBE/def2-SVP (**3**) levels of theory. Important for these structures is selecting a suitable fragment of the crystal and correct multiplicities for Cu d^9 to capture the full structure and avoid correlation errors from broken bonds. For **1** the selected fragment was $[Cu(SO_4)_6]^{10-}$, for **2** $[Cu_2(OH_2)(SO_4)_5]^{6-}$, for **3** $[Cu(OH_2)_3(SO_4)]$ and for **4** $[Cu_2(OH_2)_8(SO_4)(H_2O)]^{2-}$. For the very negative clusters, it was found that B3LYP performed much better than PBE. The ORCA 5.0 software suite was employed on an i7-8700 CPU @ 3.20GHz computer with 16 Gb RAM under Windows 10.[49] NoSpherA2 was set for high accuracy partitioning. Determination of the absolute structure of the unit cell in **3**, using Bayesian statistics on Bijvoet differences in Olex2, results in a Flack parameter of -0.016(5). After a careful review of various trials, it was decided to employ distance restraints of 0.989 Å on O–H because this greatly improved the precision of these bond lengths. Free refinements on **3** and **4** closely approximated this 'best value' from neutron diffraction at 100 K but with larger s.u.[50] In the case of **2**, the crystal, and hence the data, quality were insufficient to permit refinement of the anisotropic displacements of H but the positions could be refined with accurate O–H bond distances.[50]

Conclusions

Single-crystal X-ray crystallography with HAR has provided state-of-the art crystal structures for **1** – **4**. For **3** this is the first structure that has located the H-atoms from an X-ray diffraction experiment. The structures demonstrate that *all* H atoms in *all* water molecules and aqua ligands in **2** – **4** are fully engaged in H-bonding to neighbouring aqua and sulfato oxygen acceptors. HAR using NoSpherA2 provides accurate O–H bond distances and excellent precision for the H-bonding parameters. The loss of colour on the sequential dehydration from pentahydrate **4** to anhydrous **1** is caused by lower crystal field splitting from sulfato versus aqua oxygen donors. Thereby, the red-light absorption of the aqua complexes gradually shifts into the near infra-red with increasing numbers of sulfato ligands, with the result that **1** becomes an effective window for transmission of all wavelengths of visible light, and therefore appears almost colourless.

Author Contributions

M.A.I. prepared the original crystal samples. R.T.B. undertook the crystallography and data analysis. All authors have approved the final version of the paper.

Conflicts of interest

There are no conflicts to declare.

Acknowledgements

We are grateful for ongoing funding from the Natural Sciences and Engineering Research Council (NSERC) of Canada to RTB, and especially to the University of Lethbridge and the Faculty of Arts and Science for support to M.A.I. and for purchasing the X-ray diffractometer. We thank Dr. Florian Kleemiß of Olexsys.org for helpful advice and the Rigaku Advanced Crystallography School for informative lessons on NoSpherA2.

Notes and references

‡ A reversible reaction of hydrated copper(II) sulfate, https://edu.rsc.org/experiments/a-reversible-reaction-of-hydrated-copperii-sulfate/437.article (accessed 2021-11-27).
§ An internet search of 'Why is anhydrous copper sulfate white?' results in a variety of answers, but by far the most common are variants on the following model: "Question: CuSO4.5H2O is blue in colour while CuSO4 is colourless. Why? Answer: In CuSO4.5H2O water acts as ligand as a result it causes crystal field splitting. Hence d—d transition is possible in CuSO4.5H2O and shows colour. In the anhydrous CuSO4 due to the absence of water ligand crystal field splitting is not possible and hence no colour." https://www.doubtnut.com/pcmb-questions/cuso45h2o-is-blue-in-colour-while-cuso4-is-colourless-why-48748 (accessed 2021-11-27).
§§ The most egregious case that we have found in published material is the statement: "the splitting of d-orbitals doesn't occur in case of $CuSO_4.H_2O$", in *Molecular Symmetry and Group Theory: Approaches in Spectroscopy and Chemical Reactions*, By R. C. Maurya and J. M. Mir, 2019, Walter de Gruyter. Evidently, some branches of the chemical community have lost sight of the origins of *crystal* field theory!

1 V. Karpenko and J. A. Norris, *Chem. Listy*, 2002, **96**, 997.
2 D. M. P. Mingos, *Struct. Bond*., 2019, **181**, 1.
3 G. F. Condike, *J. Chem. Educ.*, 1975, **52**, 615.
4 A. D. Harris, L. H. Kalbus, *J. Chem. Educ.*, 1979, **56**, 417.
5 R. Barlag and F. Nyasulu, *J. Chem. Educ*. 2011, **88**, 643.
6 C. E. Housecroft and A. G. Sharpe, *Inorganic Chemistry*, 4th Ed., 2012, Pearson, p. 766.
7 M. Wildner and G. Giester, *Mineral. Petrol.*, 1988, **39**, 201.
8 G. Giester, *Mineral. Petrol.*, 1988, **38**,277.
9 R. F. Zahrobsky and W. H. Baur, 1965, *Naturwischensch.*, 1965, **52**, 389; R. F. Zahrobsky, W. H. Baur, *Acta Crystallog.*, 1968, B**24**, 508.
10 G.E. Bacon, D.H. Titterton, *Z. Kristallogr.*, 1975, **141**, 330.
11 I. B. Bersuker, *Coor. Chem. Rev.*, 2001, **101**, 1067.
12 V. P. Ting, P. F. Henry, M. Schmidtmann, C. C. Wilson, M. T. Weller, *Chem. Comm*., 2009, 7527.
13 S. Ulutan, A. P. T. Demir, D. Balkose, *Ind. Eng. Chem. Res.*, 2020, **59**, 9939.
14 X. Fu, G. Yang, J. Sun, J. Zhou, *J. Phys. Chem. A*, 2012, **116**, 7314.

15 M. T. Ruggiero, T. Bardon, M. Strlic, P. F. Taday, T. M. Korter, *J. Phys. Chem. A*, 2014, **118**, 10101; M. T. Ruggiero, T. Bardon, M. Strlic, P. F. Taday, T. M. Korter, *J. Phys. Chem. Chem. Phys. A*, 2015, **17**, 9326.
16 H. Langfelderova, *J. Therm. Anal.*, 1994, **41**, 955.
17 W-L. Ng, C-C. Ho, S-K Ng, *Inorg. Nucl. Chem.*, 1978, **34**, 459.
18 R. L. White, *Thermochim. Acta*, 2012, **528**, 58.
19 A. Sivakumar, S. S. J. Dhas, J. E. M. Theras, M. Jose, P. Sivaprakash, S. Arumugam, S. A. M. B. Dhas, *Sol. State Sci.*, 2021, **121**, 106751:1-6.
20 G. D. Ilyushin, *Rus. J. Inorg. Chem.*, 2015, **60**, 1734.
21 F. C. Hawthorne, *Mineralog. Mag*., 2014, **78**, 957.
22 R. C. Peterson, J. M. Hammarstrom, R. R. Seal II, *Amer. Mineralog*., 2006, **91**, 261.
23 J. L. Jambor, D. K. Nordstrom, C. N. Alpers, *Rev. Mineral. Geochem*., 2000, **40**, 303.
24 F. C. Hawthorne, S. V. Krivovichev and P. C. Burns, *Rev. Mineral. Geochem*., 2000, **40**, 1.
25 A. H. Compton, *Nature (London)*, 1915, **95**, 343.
26 M. Woínska, S. Grabowsky, P. M. Dominiak, K. Wózniak and D. Jayatilaka, *Sci. Adv.*, 2016, **2**, e1600192.
27 G. E. Bacon, *Neutron Diffraction*, 3rd Ed., Clarendon Press, 1975.
28 D. T. Cromer and J. T. Waber, *International tables for X-ray crystallography*, 1974, vol. IV, 71.
29 B. Dittrich and D. Jayatilaka, *Acta Crystallogr., Sect. A: Found. Crystallogr*., 2008, **64**, 383.
30 F. Kleemiss, O. V. Dolomanov, M. Bodensteiner, N. Peyerimhoff, L. Midgley, L. J. Bourhis, A. Genoni, L. A. Malaspina, D. Jayatilaka, J. L. Spencer, F. White, B. Grundkötter-Stock, S. Steinhauer, D. Lentz, H. Puschmann S. Grabowsky, *Chem. Sci.*, 2021, **12**, 1675.
31 O. V. Dolomanov, L. J. Bourhis, R. J. Gildea, J. A. K. Howard and H. Puschmann, *J. Appl. Cryst.*, 2009, **42**, 339.
32 L . J. Bourhis, O. V. Dolomanov, R. J. Gildea, J. A. K. Howard, H. Puschmann, *Acta Crystallogr., Sect. A: Found. Crystallogr*. 2015, A**71**, 59.
33 H. Ohtaki, T. Yamaguchi, M. Maeda, *Bull. Chem. Soc. Jap.*, 1976, **49**, 701.
34 M. Magini, *Inorg. Chem.*, 1982, **21**, 1535.
35 M. A. Hitchman, W. Maaskant, J. van der Plas, C. J. Simmons, and H. Stratemeier, *J. Am. Chem. Soc.*, 1999, **121**, 1488.
36 T. S. Loblana, R. Sultana, R. J. Butcher, *Dalton Trans.*, 2011, **40**, 11382.
37 I. Kita, S. Matsuo, *J. Phys. Chem.*, 1981, **85**, 792.
38 Jeffrey, G. A. *An introduction to hydrogen bonding*. Oxford University Press: New York, 1997, Vol.12, pp 330.
39 T. Steiner, *Angew. Chem. Int. Ed.*, 2002, **41**, 48.
40 S. J. Gabrowski, Hydrogen Bond – Definitions, Criteria of Existence and Various Types. In: *Understanding Hydrogen Bonds: Theoretical and Experimental Views*. Royal Society of Chemistry, 2020, pp. 1.
41 D. Götz, K. Heinzinger and A. Klemm, *Z. Naturforsch*., 1975, A**30**, 1667.
42 S. J. Louisnathan, R. J. Hill, G. V. Gibbs, *Phys. Chem. Minerals*, 1977, **1**, 53.
43 G. J. Redhammer, L. Koll, M. Bernroider, G. Tippelt, G. Amthauer and G. Roth, *Amer. Mineral.* 2007, **92**, 532.
44 M. Wildner, G. Giester, M. Kersten. K. Langer, *Phys. Chem. Minerals*, 2014, **41**, 669.
45 T. Ishii, S. Tsuboi, S. Yukinari, G. Sakane, M. Yamashita, B. K. Breedlove, *Int. J. Quant. Chem.* 2009, **109**, 2734.
46 P. M. Gruzensky, *J. Res. Nat'l. Bur. Stand. A. Phys. Chem.*, 1964, **54**A, 313.
47 G. M. Sheldrick, *Acta Cryst.* 2015, A**71**, 3.
48 C. F. Macrae, I. Sovago, S. J. Cottrell, P. T. A. Galek, P. McCabe, E. Pidcock, M. Platings, G. P. Shields, J. S. Stevens, M. Towler and P. A. Wood, *J. Appl. Cryst*., 2020, **53**, 226.
49 F. Neese, *Wiley Interdiscip. Rev.: Comput. Mol. Sci.*, 2012, **2**, 73; F. Neese, *Wiley Interdiscip. Rev.: Comput. Mol. Sci.*, 2017, **8**, e1327.
50 F. H. Allen and I. J. Bruno, *Acta Cryst. Sect. B Struct. Sci*., 2010, B**66**, 380.

ARTICLE